MobIntel: Passive Outdoor Localization via RSSI and Machine Learning

Fanchen Bao, Stepan Mazokha, Jason O. Hallstrom
I-SENSE
Florida Atlantic University
Boca Raton, FL, USA
{fbao2015, smazokha2016, jhallstrom}@fau.edu

***Abstract*—Effective planning requires understanding the movement patterns of pedestrians and vehicles. This can be achieved by passive localization of WiFi-enabled devices using RSSI measurements from WiFi probe requests received at nearby sensors. In this paper, we continue our work on a mobility intelligence system (MobIntel) [1] and study the performance of two broad approaches to RSSI-based passive outdoor localization. The first is adapted from traditional active localization methods, including multilateration and fingerprinting. The second relies on machine learning methods, including machine learning-boosted multilateration and classification. We compare the localization performance of the two approaches and find that the machine learning methods consistently outperform the adapted traditional methods. The results demonstrate machine learning methods as promising tools for RSSI-based passive outdoor localization.**

***Index Terms*—Mobility intelligence, passive localization, WiFi probe requests, RSSI**

I. Introduction

Monitoring mobility patterns of pedestrians and vehicles provides vital information for city planning. This can be achieved by passive localization using received signal strength indicator (RSSI) measurements from probe requests emitted by WiFi-enabled devices. We consider two modes of RSSI-based localization: active and passive [2]. The former requires device cooperation, whereas the latter does not. Active localization may not be suitable to a city, as it typically requires large-scale mobile app adoption. Thus, passive localization is preferred.

One challenge in RSSI-based localization is high variability in RSSI measurements [3]. Some active localization approaches address this by requiring devices to transmit additional information, such as round-trip time [4] or device orientation [5]. However, these data points are not available in passive localization. Others have shown that active localization is possible using only RSSI measurements from access points (APs) [6]. Given its resemblance to passive localization, these approaches might be transferable. However, transferability must be verified due to inherent differences between active and passive localization. For instance, active localization can handle missing RSSI measurements by collecting them again, yet this is not always possible in passive localization.

Previous work on passive localization handles only small- or large-scale applications (Section II-B). This leaves opportunity for a solution targeting the medium scale, such as a city street. Therefore, it is necessary to examine the feasibility of adapting *active* localization methods (hereafter referred to as "traditional active localization methods") to the passive context, and to explore new approaches to RSSI-based passive localization in outdoor environments.

To facilitate this goal, we have developed a privacy-centric system, MobIntel, to capture and analyze RSSI measurements from anonymized WiFi probe requests. In this paper, our contributions include: 1) a systematic performance analysis of RSSI-based passive outdoor localization methods for medium-scale application adapted from traditional active localization (multilateration and fingerprinting); and 2) a systematic analysis of the accuracy impact of integrating machine learning within these methods.

II. Related Work

We present a brief review of related work in both active and passive RSSI-based localization. Emphasis is given to applicability issues related to the scale of a city street.

A. Active Localization

Multilateration is commonly used in active localization. It employs an RSSI-distance model to estimate distances from target devices to nearby APs, and then applies linear least squares regression to estimate the most likely location of the device. Most research focuses on improving the RSSI-distance model. Some approaches add additional information to mitigate RSSI variability, such as the WiFi fine timing measurement frame [4]. However, these approaches typically require cooperation from the target device. Others drop RSSI completely and use measurements such as RF signal angle-of-arrival or time-of-arrival to yield higher multilateration accuracy [7]. Yet, collecting these measurements requires specialized tools, whose cost and complexity are at odds with large-scale deployment and maintenance on a city street. Therefore, a more desirable way to leverage multilateration is to adapt an RSSI-based method to passive localization.

Another common method in active localization is based on *fingerprinting*. In the offline stage, a radio map is constructed from RSSI measurement vectors (i.e., fingerprints) that originate from nearby APs and are captured by a testing device at each reference point. In the online stage, RSSI measurements collected by a target device are compared to the fingerprints, and the reference point with the best match is the predicted location. Radio map quality can be improved by including additional information, such as device azimuth [5].

978-1-6654-2854-5/21/$31.00 ©2021 IEEE

Similar to multilateration, fingerprinting is adaptable to passive localization if cooperative measurements are not used to construct the radio map. One challenge is that radio map construction scales poorly in large outdoor environments because to achieve sufficient granularity, many reference point measurements are needed. In active localization, this can be alleviated via crowdsourcing, as RSSI fingerprints can be easily collected and uploaded by any device [8]. Yet, this is not the case with passive localization, since the radio map is not constructed from mobile devices, but sensors. This means the targets of crowdsourcing would be local, stationary WiFi devices (e.g., public or private APs) that agree to volunteer as sensors. Finding such volunteers and retrieving data from them is likely to be challenging.

B. Passive Localization

Disturbance-based passive localization can track any object, including non-RF objects, in a small area surrounded by APs [9]. The APs constantly send beacons and collect baseline RSSI measurements from other beacons. When an object enters the AP-covered area, the disturbance pattern in RSSI measurements reveals the location of the intruding object. Unfortunately, this method is not scalable to a large outdoor area because the number of objects that can be tracked simultaneously is low. If too many objects (e.g., pedestrians) are present in the AP-covered area, the disturbance pattern will be too chaotic to be informative.

Another type of passive localization leverages WiFi probe requests in a qualitative manner. Guillen-Perez and Cano [10] propose that a target device can be assigned the same location as the sensor that captured its probe request with the strongest signal. It is suitable on a large scale, but too imprecise for a city street. Resolution can be enhanced with more sensors, but this would incur scalability issues. Kulshrestha et al. [11] temporarily improve the resolution of qualitative passive localization by attaching sensors to volunteers and having them move in the same general direction as target devices. However, this is not a generalized or long-term solution.

Overall, these passive localization methods cannot meet the requirements of mobility monitoring on a city street. A more appropriate method should leverage routing traffic sent by devices (e.g., probe requests), as the alternative RSSI-disturbance-based methods are inappropriate at scale. Quantitative methods are preferred, because qualitative methods either lack or cannot sustain long-term precision.

III. Methods

In this section, we describe our approaches to enabling RSSI-based passive localization, including adaptation of traditional multilateration and fingerprinting methods, and formulation of machine learning-boosted multilateration and classification methods.

A. Multilateration

Adapting traditional multilateration methods to passive localization requires that the RSSI measurements be obtained by sensors instead of target devices. The basic RSSI path-loss model (Equation (1)) is used, where R is the RSSI measurement, d is the distance between sensor and target device, A is RSSI measured at a reference distance from the device (usually 1 m), and n is the mean, environment-specific path-loss index that describes the rate of signal loss with distance [12]. In a stable environment, A and n are constants. Therefore, the relation between R and $\log(d)$ can be captured by linear regression.

$$R = A - 10n \log(d) \tag{1}$$

Once device-to-sensor distances are estimated, they are sent to a least squares estimator to find the coordinates $(\hat{x}, \hat{y})$ that minimize the residual error shown in Equation (2), where d_i is the estimated distance from the target device to the i-th sensor, and (x_i, y_i) are the coordinates of the i-th sensor.

$$\text{Residue} = \sum_{i=1}^{N} \left(d_i - \sqrt{(x_i - \hat{x})^2 + (y_i - \hat{y})^2} \right)^2 \tag{2}$$

B. Fingerprinting

Similar to multilateration, adapting fingerprinting to the passive context entails switching how RSSI measurements are collected. The radio map is constructed from vectors of RSSI measurements, with each vector corresponding to a reference point and consisting of the mean RSSI measurements from each sensor [13]. Suppose there are N sensors S_1, S_2, ..., S_N, M reference points P_1, P_2, ..., P_M, and all reference points are within the detection range of all sensors. RSSI measurements obtained by a sensor S_j $(1 \leq j \leq N)$ at reference point P_i $(1 \leq i \leq M)$ can be expressed as R_{ij1}, R_{ij2}, ..., R_{ijT}, where T is the number of probe requests captured. Let μ_{ij} be the mean value of all RSSI measurements obtained by S_j at P_i. The RSSI fingerprint of P_i is $F_i = [\mu_{i1}, \mu_{i2}, ..., \mu_{iN}]$.

Given RSSI measurements $U = [R'_1, R'_2, ..., R'_N]$ acquired from a target device at an unknown location, the matching penalty between U and F_i can be approximated by Euclidean distance. The smaller the distance, the more likely U and F_i originate from the same P_i. In practice, reference points of the top k best matches are averaged to compute the predicted location, with k determined via cross validation.

C. Machine Learning-boosted Multilateration

In multilateration, the RSSI path-loss model (Equation (1)) does not capture all errors [14]. While it is possible to attach more error terms to the model, a less complex approach is to let a machine learning architecture "learn" the relation between RSSI measurements and distances. Machine learning offers an advantage in that it is not constrained by a physical model and is thus able to handle non-ideal scenarios. We use three standard machine learning architectures: multi-layer perceptron (MLP), support vector machine (SVM), and k-nearest neighbors (K-NN) to train an RSSI-distance regressor for each sensor. Each regressor is used in multilateration the same way as described in Section III-A.

D. Machine Learning Classification

The high-level fingerprinting workflow involves passing RSSI measurements to a radio map-based algorithm that predicts a target location. This process can be achieved through machine learning classification, where RSSI measurements are the features, and the reference points are the labels. The difference between fingerprinting and classification is that the former has predefined rules regarding how RSSI measurements match reference points (e.g., Euclidean distance), whereas the latter "learns" the matching process from the data. We again use three machine learning architectures (MLP, SVM, and K-NN) to train the classifiers.

IV. Data Collection

To examine the localization performance of the methods discussed above, RSSI measurements from mock probe requests and reference point coordinates were collected in a semi-controlled environment. In the following sections, the data collection and preparation procedures are presented.

A. Experimental Design

Figure 1(A) shows our 15×15 m experimental field, divided into 1×1 m cells. Red dots denote sensor locations; blue dots denote reference points. Figure 1(B) shows the actual obstacle-free field (GPS: 26.381488, -80.099640). During data collection, sensors were mounted on tripods approximately 1.8 m above the ground. An emitter, mounted on a tripod approximately 1 m above the ground, was placed on each reference point for 50 seconds, during which time approximately one-thousand mock probe requests were sent. Each mock probe request carries a MAC address that is traceable to the reference point, distinguishable from a genuine probe request, and unique. The RSSI measurement and the mock probe request timestamp were uploaded to an AWS store by each sensor.

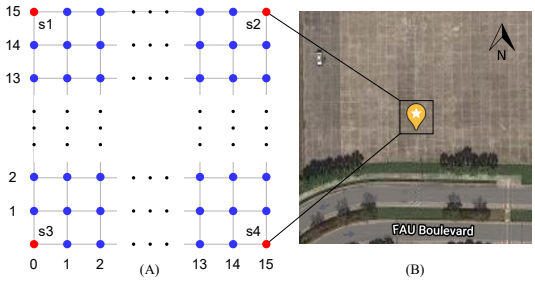

Fig. 1: Experimental Design and Satellite View of Experimental Field

B. Hardware - Sensor

The same sensing device described in [1] was used in this paper. Briefly, the sensor captures WiFi probe requests, removes duplicates for each 30-second window, and uploads the aggregated data to AWS.

C. Hardware - Emitter

The same device used for stress testing in [1] was used as the emitter. It sends WiFi probe requests with a customized MAC address, on a specified channel, and at a specified rate.

D. Data Preparation

Raw data was collected on 07/16/2020. Due to the nature of passive localization, missing data in RSSI measurements is not uncommon. Here, missing data refers to a situation where a probe request is not captured by every sensor, despite all sensors being within the normal detection range. Since analyzing the effect of missing data is outside the scope of this paper, we only use raw data with full RSSI measurements to derive multiple datasets for analysis. Figure 2 illustrates the relationships among the derived datasets, with their names, number of rows, and derivation methods.

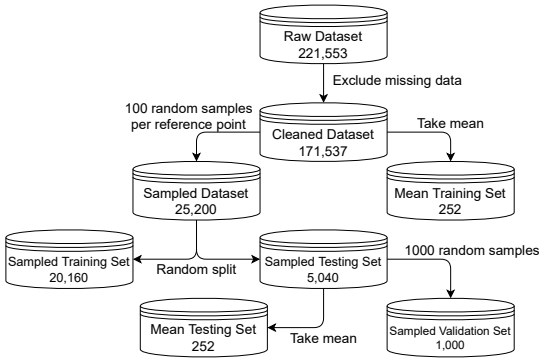

Fig. 2: Relationships Among Datasets

The sampled and mean training sets are used to train **sampled models** and **mean models**, respectively. Given that taking the mean of RSSI measurements reduces random error [3], but also shrinks sample size, it is interesting to see how mean model performance compares to sampled model performance.

V. Traditional Methods

We adapt multilateration and fingerprinting to passive localization and analyze the resulting performance. Localization performance is visualized by the cumulative distribution function (CDF) of localization error, which is defined as the Euclidean distance between the predicted and true coordinates of a test observation. Generally speaking, the larger the area-under-the-curve, the better the performance.

A. Multilateration

The sampled and mean RSSI path-loss models are generated by linear regression for each sensor based on Equation (1). Table I shows the error metrics when evaluated on the sampled testing set. R^2 describes the variance in the training data explainable by the path-loss model, and mean absolute error (MAE) describes the error of distance prediction. Within each sensor, the sampled and mean models exhibit almost identical performance. Across models for different sensors, s_4 exhibits the best performance, whereas s_1 the worst. A possible explanation is that a source of interference may be present on the northwest corner of the experimental field, which affects s_1 the most, and s_4 the least. A likely candidate of such interference is the local airport, which is located about 650 m to the northwest of the experimental field.

TABLE I: Metrics of Path-loss [12] Models on the Sampled Testing Set

Sensor	Sampled		Mean	
	R^2	MAE	R^2	MAE
s_1	0.61	4.62	0.61	4.63
s_2	0.65	4.06	0.65	4.07
s_3	0.61	4.03	0.61	4.03
s_4	0.71	3.44	0.71	3.46

The sampled and mean multilateration models are produced from the sampled and mean RSSI path-loss models, respectively. Figure 3(A) summarizes their performance when evaluated on different testing sets. The x-axis denotes localization error, and the y-axis denotes the probability that a model's error is less than or equal to the error value. The blue, orange, and green curves represent the performance of three scenarios: (1) the sampled model tested on the sampled testing set (sampled-sampled), (2) the mean model tested on the sampled testing set (mean-sampled), and (3) the mean model tested on the mean testing set (mean-mean), respectively.

The sampled-sampled curve overlaps the mean-sampled curve, illustrating similar performance between the two scenarios. The mean-mean curve shows slightly better performance than the other two, but this is likely an artifact due to the similarity between the mean training and testing sets. Recall that the mean training set derives from the cleaned dataset, and the mean testing set from the sampled testing set (Figure 2). Since the sampled testing set is a subset of the cleaned dataset, there is information overlap between the mean testing and training sets. This inflates the observed mean-mean performance.

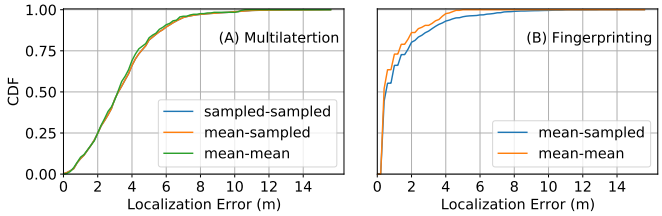

Fig. 3: CDF of Error with Traditional Methods [4, 13]

B. Fingerprinting

The radio map for fingerprinting is a 252×4 matrix prepared from the mean training set. We determine k as follows: A series of fingerprinting models, constructed via k-nearest neighbors, with k ranging from 1 to 20, are examined on the sampled validation set consisting of 1,000 observations from the sampled testing set (Figure 2). We find that $k = 2$ results in the least validation error, defined as the root mean squared localization error [13]. With $k = 2$, the performance of fingerprinting is shown in Figure 3(B). The CDF layout is the same as described earlier. The blue and orange curves represent localization performance on the sampled and mean testing sets, respectively. The sampled validation set is not included in the sampled testing set during evaluation. Similar to traditional multilateration, information overlap between the mean testing and training sets likely yields inflated mean-mean performance.

VI. Machine Learning Methods

Machine learning-boosted multilateration and classification methods are evaluated using three architectures—MLP, SVM, and K-NN. Each is trained to produce a sampled and mean model. Hyperparameter tuning for each model is conducted via two rounds of cross-validation. For the sampled model, five-fold cross-validation is used. For the mean model, multi-fold cross-validation is not feasible due to lack of data redundancy in the mean training set; hence, all tuning is conducted on the sampled validation set. After tuning, the finalized hyperparameters are used to re-train the model before evaluation.

A. Machine Learning-boosted Multilateration

In machine learning-boosted multilateration, we replace the RSSI path-loss model with a machine learning-based RSSI-distance regressor. Table II lists the R^2 and MAE values for the regressors when evaluated on the sampled testing set. Within each architecture, the sampled and mean models show similar regression performance. Across architectures, there is also little difference separating the sampled and mean models. Across the sensors, s_4 has the lowest error, whereas s_1 has the highest. This mirrors the findings in the path-loss model evaluation. Overall, the machine learning-based RSSI-distance regressors outperform the path-loss model in distance estimation; the regressors reduce MAE by half, while maintaining similar R^2 scores.

Each regressor is then used to build a machine learning-boosted multilateration model, as described in Section V-A. The localization performance is demonstrated in Figures 4(A), (B), and (C). Within each architecture, all three CDF curves illustrate similar performance. This is not surprising given the similar RSSI-distance regression performance. The slightly better performance from the mean-mean curve is likely an artifact, as explained earlier.

We also compare the performance of the best CDF curves across all three architectures, with the mean-mean curve excluded. The results are shown in Figure 4(D). There is no clear winner among the three curves.

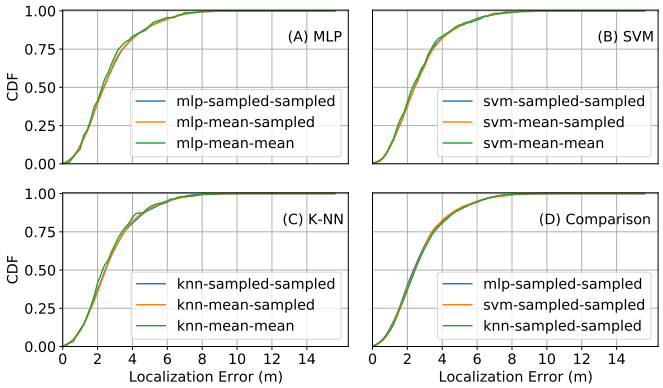

Fig. 4: CDF of Error with Machine Learning-boosted Multilateration

B. Machine Learning Classification

The localization process based on machine learning classification mimics that of fingerprinting, except that the Euclidean

TABLE II: Metrics of Machine Learning-based RSSI-Distance Regressors Evaluated on the Sampled Testing Set

	MLP				SVM				K-NN			
	Sampled		Mean		Sampled		Mean		Sampled		Mean	
Sensor	R^2	MAE	R^2	MAE	R^2	MAE	R^2	MAE	R^2	MAE	R^2	MAE
s_1	0.53	2.48	0.52	2.50	0.53	2.45	0.53	2.47	0.52	2.48	0.53	2.48
s_2	0.64	2.05	0.64	2.05	0.63	2.05	0.63	2.06	0.63	2.12	0.64	2.07
s_3	0.57	2.39	0.56	2.40	0.56	2.35	0.55	2.36	0.57	2.39	0.56	2.44
s_4	0.68	1.92	0.67	1.93	0.67	1.89	0.66	1.92	0.67	1.89	0.67	1.92

distance-based matching penalty is replaced by penalties learned directly from the data. Table III summarizes the true and "adjacent" accuracy of each machine learning classifier evaluated on the sampled testing set. True accuracy reflects the proportion of test observations whose labels were correctly predicted. Adjacent accuracy reflects the proportion of testing observations whose predicted labels either matched the true labels or one of the eight surrounding labels. Since adjacent accuracy is above 80%, it means even when the prediction is wrong, it is usually only slightly off target. Within each architecture, the sampled model has slightly better classification performance than the mean model. Across architectures, MLP has the worst classification performance, whereas SVM and K-NN perform similarly.

TABLE III: True and Adjacent Accuracy of Machine Learning Classifiers

	MLP		SVM		K-NN	
Accuracy	Sampled	Mean	Sampled	Mean	Sampled	Mean
True	0.63	0.55	0.70	0.68	0.69	0.68
Adjacent	0.81	0.78	0.84	0.83	0.84	0.80

Localization performance of all three architectures is summarized in Figures 5(A), (B), and (C). Within each architecture, the sampled-sampled curve reflects slightly better performance than the mean-sampled curve, but they are both dwarfed by the mean-mean curve. The exceptional performance represented by the mean-mean curve is most likely an artifact as discussed previously. However, overall performance also appears exaggerated. This is due to the nature of classification, where a correct match automatically yields 0 m error, inflating the CDF curve.

The best CDF curves across all three architectures are also compared, with the mean-mean curves excluded. The result is shown in Figure 5(D), where SVM performs slightly better than the others.

VII. Battle Royal

To compare localization performance across all methods, the best CDF curve for each method, excluding the mean-mean curves, are placed in the same plot (Figure 6). The blue, orange, green, and red curves correspond to multilateration (sampled-sampled), fingerprinting (mean-sampled), machine learning-boosted multilateration (mlp-sampled-sampled), and classification (svm-sampled-sampled), respectively. A few observations can be made.

First, the machine learning models outperform their traditional counterparts. This is not surprising, as machine learning methods are free to interpret data that might be ignored or not

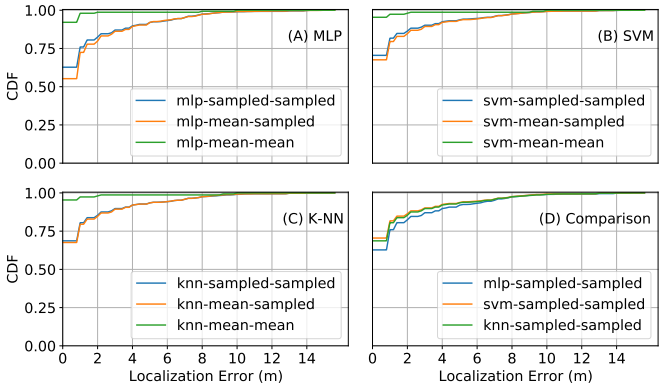

Fig. 5: CDF of Error with Machine Learning Classification

properly modeled in the traditional methods. Second, the best non-multilateration method outperforms the best multilateration method by a large margin. This is most likely due to multilateration requiring two rounds of estimation, compared to one round in other methods. Third, except for fingerprinting, all Battle Royal CDF curves are sampled-sampled, which means the sampled models either outperform, or perform as well as the mean models. This answers the question raised in Section IV-D: The benefit of reduced random error in the mean training set does not outweigh the cost of reduced sample size. Finally, the best performing method (i.e., machine learning classifier) exhibits above 90% probability of achieving an error below 3 m. This resolution is sufficient to tell that a device has moved from one business to another on a city street.

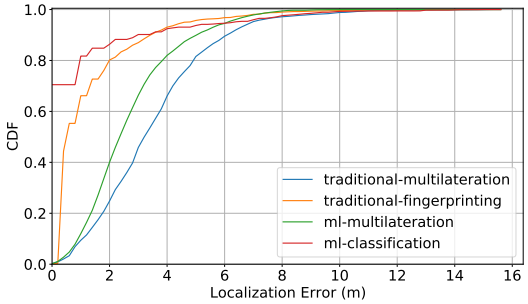

Fig. 6: Comparison of Localization Error Among All Methods

VIII. Conclusion

In this paper, we have systematically evaluated the performance of two traditional active localization methods adapted for use in passive localization, along with their machine learning-boosted counterparts. The results show that the machine learning methods perform better than the adapted tra-

ditional methods. In particular, the SVM sampled classifier appears to have sufficient resolution for mobility monitoring in typical urban environments. However, several limitations need to be addressed in future research.

First, all models are trained and tested on the data collected in the same session. To demonstrate that a model possesses temporal robustness, it must be evaluated on data collected across different sessions and retain performance.

In addition, data in this paper was collected in an obstruction-free environment and only those with no missing data were included in the analysis. This is not representative of city streets, as signal noise and RSSI measurement loss are inevitable. Thus, future research will investigate how model performance deteriorates when data collection is not ideal.

Finally, all models trained are based on inputs from exactly four sensors. This presents a scalability issue, where change in sensor count would require re-training of the model. Given that scaling sensors up or down is common in practice, future research will focus on generating a scalable model, whose performance is resilient to small changes in sensor availability.

IX. Acknowledgement

This research is supported by the City of West Palm Beach, the Knight Foundation, and the Community Foundation of Palm Beach and Martin Counties. We'd like to thank Chris Roog, Executive Director of the Community Redevelopment Agency in the City of West Palm Beach for his continued assistance in MobIntel; and thank the Florida Atlantic University *I-SENSE* team for hardware and logistics support.

References

[1] S. Mazokha, F. Bao, J. Zhai, and J. Hallstrom, "MobIntel: sensing and analytics infrastructure for urban mobility intelligence," in *2020 IEEE International Conference on Smart Computing (SMARTCOMP) (SMARTCOMP 2020)*, Bologna, Italy, Italy, Jun. 2020.

[2] L. Sun, S. Chen, Z. Zheng, and L. Xu, "Mobile Device Passive Localization Based on IEEE 802.11 Probe Request Frames," *Mobile Information Systems*, vol. 2017, pp. 1–10, 2017. [Online]. Available: https://www.hindawi.com/journals/misy/2017/7821585/

[3] W. Xue, W. Qiu, X. Hua, and K. Yu, "Improved Wi-Fi RSSI Measurement for Indoor Localization," *IEEE Sensors Journal*, vol. 17, no. 7, pp. 2224–2230, Apr. 2017, conference Name: IEEE Sensors Journal.

[4] G. Guo, R. Chen, F. Ye, X. Peng, Z. Liu, and Y. Pan, "Indoor Smartphone Localization: A Hybrid WiFi RTT-RSS Ranging Approach," *IEEE Access*, vol. 7, pp. 176 767–176 781, 2019, conference Name: IEEE Access.

[5] N.-S. Duong and T.-M. Dinh, "Indoor Localization with lightweight RSS Fingerprint using BLE iBeacon on iOS platform," in *2019 19th International Symposium on Communications and Information Technologies (ISCIT)*, Sep. 2019, pp. 91–95, iSSN: 2643-6175.

[6] J. Wang, J. Luo, S. J. Pan, and A. Sun, "Learning-Based Outdoor Localization Exploiting Crowd-Labeled WiFi Hotspots," *IEEE Transactions on Mobile Computing*, vol. 18, no. 4, pp. 896–909, Apr. 2019, conference Name: IEEE Transactions on Mobile Computing.

[7] X. Li, Z. D. Deng, L. T. Rauchenstein, and T. J. Carlson, "Contributed Review: Source-localization algorithms and applications using time of arrival and time difference of arrival measurements," *Review of Scientific Instruments*, vol. 87, no. 4, p. 041502, Apr. 2016, publisher: American Institute of Physics. [Online]. Available: https://aip.scitation.org/doi/10.1063/1.4947001

[8] H. Du, C. Zhang, Q. Ye, W. Xu, P. L. Kibenge, and K. Yao, "A hybrid outdoor localization scheme with high-position accuracy and low-power consumption," *EURASIP Journal on Wireless Communications and Networking*, vol. 2018, no. 1, p. 4, Jan. 2018. [Online]. Available: https://doi.org/10.1186/s13638-017-1010-4

[9] M. Youssef, M. Mah, and A. Agrawala, "Challenges: device-free passive localization for wireless environments," in *Proceedings of the 13th annual ACM international conference on Mobile computing and networking*, ser. MobiCom '07. New York, NY, USA: Association for Computing Machinery, Sep. 2007, pp. 222–229. [Online]. Available: https://doi.org/10.1145/1287853.1287880

[10] A. Guillen-Perez and M.-D. Cano, "Counting and locating people in outdoor environments: a comparative experimental study using WiFi-based passive methods," *ITM Web of Conferences*, vol. 24, p. 01010, 2019, publisher: EDP Sciences. [Online]. Available: https://www.itm-conferences.org/articles/itmconf/abs/2019/01/itmconf_amcse18_01010/itmconf_amcse18_01010.html

[11] T. Kulshrestha, D. Saxena, R. Niyogi, and J. Cao, "Real-Time Crowd Monitoring Using Seamless Indoor-Outdoor Localization," *IEEE Transactions on Mobile Computing*, vol. 19, no. 3, pp. 664–679, Mar. 2020, conference Name: IEEE Transactions on Mobile Computing.

[12] F. Shang, W. Su, Q. Wang, H. Gao, and Q. Fu, "A Location Estimation Algorithm Based on RSSI Vector Similarity Degree," *International Journal of Distributed Sensor Networks*, vol. 10, no. 8, p. 371350, Aug. 2014, publisher: SAGE Publications. [Online]. Available: https://doi.org/10.1155/2014/371350

[13] S. Yiu, M. Dashti, H. Claussen, and F. Perez-Cruz, "Wireless RSSI fingerprinting localization," *Signal Processing*, vol. 131, pp. 235–244, Feb. 2017. [Online]. Available: http://www.sciencedirect.com/science/article/pii/S0165168416301566

[14] Z. He, Y. Li, L. Pei, R. Chen, and N. El-Sheimy, "Calibrating Multi-Channel RSS Observations for Localization Using Gaussian Process," *IEEE Wireless Communications Letters*, vol. 8, no. 4, pp. 1116–1119, Aug. 2019, conference Name: IEEE Wireless Communications Letters.